

Achievement of FCC specification in critical current density for Nb₃Sn superconductors with artificial pinning centers

X Xu¹, X Peng², J Rochester³, M Sumption³ and M Tomsic²

¹Fermi National Accelerator Laboratory, Batavia, IL 60510, U.S.A

²Hyper Tech Research Incorporated, 539 Industrial Mile Road, Columbus, OH 43228, U.S.A

³Department of MSE, the Ohio State University, Columbus, OH 43210, U.S.A

E-mail: xxu@fnal.gov

Abstract

In this letter we demonstrate achievement of record non-Cu critical current density ($J_{c,non-Cu}$) in ternary, multifilamentary Nb₃Sn conductors by the introduction of artificial pinning centers (APC). In the past two years, we have made great progress in the development of APC Nb₃Sn wires. Recent resistivity vs magnetic field measurements confirmed the high upper critical field (B_{c2}) of ternary APC wires, which at 4.2 K was ~28 T, about 1-2 T higher than present state-of-the-art conductors. In addition to high B_{c2} , it was found that APC wires have noticeably higher Sn content in the Nb₃Sn layers as compared to standard wires, which can be explained using a recent diffusion reaction theory. The $J_{c,non-Cu}$ values of the most-recent APC wires have broken the Nb₃Sn $J_{c,non-Cu}$ record that stood for nearly two decades and have met the $J_{c,non-Cu}$ specification required by the Future Circular Collider (FCC), with the best heat treatment leading to a $J_{c,nonCu}$ 29% higher than the FCC specification at 21 T. Microscopy analysis shows that the APC wires still have overly high residual Nb fractions due to too low of a Sn/Nb ratio, indicating that there is still great potential for further $J_{c,non-Cu}$ improvement. The development of APC wires is ongoing; this letter details some of the steps forward in the optimization and lays out a roadmap to push the APC wires towards practical, magnet-grade conductors.

Keywords: Nb₃Sn Superconductor, Artificial pinning center, B_{c2} , J_c .

1. Introduction

The proposed High-Energy Large Hadron Collider (HE-LHC) upgrade as well as Future Circular Collider (FCC) aims to push the energy frontier for high energy physics, and both require thousands of 16 T dipoles based on Nb₃Sn superconductors [1]. Design studies of such magnets have been pursued in earnest for a few years using a Nb₃Sn conductor specification with non-Cu critical current density ($J_{c,non-Cu}$) no less than 1500 A/mm² at 4.2 K and 16 T [2,3]. Conductor $J_{c,non-Cu}$ is a critical factor for such large machines because building 16 T magnets with conductors of lower $J_{c,non-Cu}$ would require a larger coil size and thus significantly increase the overall project cost. However, even the record $J_{c,non-Cu}$ achieved by the very top-performing rod-restack-process (RRP) wires, which are the present state-of-the-art Nb₃Sn conductors, is 10-15% below the FCC conductor $J_{c,non-Cu}$ specification [4,5]. Furthermore, this record $J_{c,non-Cu}$ level cannot be maintained in series productions because of the inevitable $J_{c,non-Cu}$ spread among billets: a ~30% variation is seen in the RRP conductors for the High-Luminosity LHC (HL-LHC) upgrade [4,5], which means that in fact a ~45-50% improvement in $J_{c,non-Cu}$ is needed to fulfill the FCC $J_{c,non-Cu}$ requirement with a reasonable conductor acceptance fraction. This is a huge challenge considering that the record $J_{c,non-Cu}$ of Nb₃Sn conductors has been at a plateau since the early 2000s [6] despite extensive efforts to break this barrier.

There are three factors determining the $J_{c,non-Cu}$ of a uniform Nb₃Sn wire: (1) fine-grain (FG) Nb₃Sn area fraction within subelements, (2) irreversibility field (B_{irr}), and (3) flux pinning capacity. For present state-of-the-art conductors, the first two factors are already quite close to the limits that Nb₃Sn wires can achieve [5], and the only chance for significant further improvements in the $J_{c,non-Cu}$ of Nb₃Sn conductors lies in enhanced flux pinning. The primary

flux pinning centers for all commercial Nb₃Sn conductors are the grain boundaries, the density of which can be improved by using a lower heat treatment (HT) temperature, but this usually reduces B_{irr} , making this approach counterproductive for high field applications [7]. The other way to improve flux pinning is the introduction of artificial pinning centers (APC), which in fact has long been a “holy grail” in the Nb₃Sn area. Significant efforts had been made using various techniques since the 1980s but none succeeded in producing superior J_c in wires [8-13] until 2014 when this was finally realized via the internal oxidation method [14]. This method was used in Nb₃Sn tapes in the 1960s [15] but had been believed ineffective in Nb₃Sn wires after some early unsuccessful attempts (e.g., [11,12]). About a decade later we revisited this work and were able to find out the essentials for this method to work [14], finally making this technique applicable to Nb₃Sn wires. We first demonstrated using binary monofilament wires the effects of this technique (e.g., significantly refined grain size, doubled layer J_c at 12 T despite low B_{irr} , shift of pinning force curve peak from $0.2B_{irr}$ to $0.34B_{irr}$, etc.) [14,16], and then proposed applying it in the powder-in-tube (PIT) design in order to make multi-filamentary wires [16,17]. Then binary multi-filamentary wires were fabricated by SupraMagnetics Inc. [18] and Hyper Tech Research Inc. [19], which confirmed the monofilament results. On the other hand, the low B_{irr} values seen in the binary monofilaments and multi-filamentary APC wires [16,18,19] showed the need for ternary dopants. Several groups began to study the effect of ternary doping to the APC wires from 2017, including Florida State University (FSU) [20] and University of Geneva [21], as well as a collaboration between Hyper Tech, Fermilab, and the Ohio State University (OSU) that began in earnest to develop ternary APC-PIT multifilamentary wires. As a surprising side result, FSU found in monofilaments the effect of grain refinement via Hf doping without internal oxidation, which could also be a promising method to improve Nb₃Sn J_c [20].

The joint efforts by Hyper Tech, Fermilab, and OSU have led to rapid improvement in performance of the ternary multifilamentary APC wires over the last two years. The transport resistance vs field (R - B) and voltage vs current (V - I) tests up to 31 T on the first set of ternary multifilamentary APC wires at the National High Magnetic Field Laboratory (NHMFL) in late 2018 [22] clearly demonstrated that the low B_{irr} issue seen in binary APC wires had been solved by addition of Ta dopant, which was also seen in other groups [20,21]. In fact, the B_{irr} and B_{c2} values (4.2 K) of the APC wire with 1wt.% Zr (T3882-0.84mm-675°C/330h, denoted “APC-B” in [22]) were 26.8 and 27.6 T, respectively, ~ 2 T higher than the reference RRP wire that is used for the HL-LHC project. The measured $J_{c,non-Cu}$ (4.2 K, 16 T) of T3882-0.84mm-675°C/330h had reached a similar level to that of the reference RRP wire (close to 1100 A/mm²). Scanning electron microscopy (SEM) analysis showed that the average FG Nb₃Sn area fraction in the filaments of T3882-0.84mm-675°C/330h was only 22%, while the residual Nb fraction was as high as 45%. Indeed, the FG Nb₃Sn layer J_c of T3882-0.84mm-675°C/330h was 2.5 times higher than that of the reference RRP wire at 4.2 K, 16 T (4710 vs 1870 A/mm²) [22]. This made it clear that there was still huge potential for further improvement of $J_{c,non-Cu}$ via precursor ratio optimization, which could allow more FG formation.

A second set of ternary APC wires had been developed, guided by the analysis on the first set of wires, and were tested at the NHMFL in early 2019. The results, reported here, not only confirm the high B_{irr} and B_{c2} of ternary APC wires, but also demonstrate $J_{c,non-Cu}$ which has achieved (or surpassed) the FCC specification.

2. Experimental

2.1. Samples

The APC wire used here, T3912, is based on a 48/61-filament design (i.e., 48 Nb₃Sn and 13 Cu filaments) with a Cu/non-Cu ratio of 1.3, fabricated at Hyper Tech using a Nb-1wt.%Zr-7.5wt.%Ta tube and a mixture of Cu, Sn, and SnO₂ powders. Most of the filaments of T3912 had sufficient oxygen, but the recipe was not yet fully optimized with respect to the Cu/Sn and Nb/Sn ratios, as will be discussed below. The wire was fabricated using a billet with a starting diameter of 19 mm, which was drawn to final wire diameters of 0.5, 0.71, and 0.84 mm without breakage, resulting in a total length of ~200 meters. Two commercial, state-of-the-art, Nb₃Sn wires were tested together with the T3912 samples as references: one was a Ti-doped RRP wire (billet number 00076) with a diameter of 0.85 mm and 108/127 subelements, and the other was a standard PIT wire (billet number 31284) with a diameter of 0.78 mm and 192/217 filaments; both wires were manufactured by Bruker EST and used for HL-LHC.

All wires were heat treated under vacuum. The APC wires with 0.71 mm and 0.84 mm diameters were reacted at 675°C, 685°C, and 700°C for various durations (specified below), all with a standard ramp rate of 30°C/h without intermediate steps. The RRP wire was heat treated using the HL-LHC protocol: 210°C/48h + 400°C/48h + 665°C/75h [4]. The standard PIT wire used a two-stage heat treatment 630°C/100h + 640°C/50h in order to maximize its $J_{c,non-Cu}$ while maintaining high residual resistivity ratio (RRR) [23].

2.2. Measurements

Two types of transport tests were performed on these wires at the NHMFL: (1) *R-B* measurements using a sensing current of 31.6 mA, allowing determinations of B_{c2} and B_{irr} , (2) *V-I* measurements at various fields, giving critical current (I_c) values. All tests were at 4.2 K in a 31 T magnet with fields perpendicular to the wire axes. Great care was taken to ensure that each sample was centered within the magnet. The *R-B* tests were performed on samples 15 mm in

length with a voltage tap spacing of 5 mm. Since five samples could be mounted together in the holder for each run, we always included one reference wire in order to give a double check on the results. Voltages were recorded for both increasing and decreasing fields; by using a proper time constant, hysteresis could be decreased to 0.2-0.3 T – the results shown below were for decreasing fields. The $V-I$ measurements used the I_c transport test system from the Applied Superconductivity Center (ASC) at the NHMFL (including the I_c rig, sample holders, data acquisition system, testing program, etc.), and were performed on straight samples 35 mm in length with a voltage tap separation of 6 mm. A criterion of 0.1 $\mu\text{V}/\text{cm}$ was used to determine the I_c values.

Samples for back-scattered electron (BSE)/SEM studies were mounted in conductive Bakelite powder and polished to 0.05 μm . The compositions of the Nb_3Sn layers were measured using energy-dispersive spectroscopy (EDS): 25 kV was used for the accelerating voltage, with an EDS count rate above 40000 counts per second, and for each spot data were collected for 30 seconds.

3. Measurement results

The $R-B$ curve of T3912 (0.84 mm diameter given a HT of 675°C/384h) is shown in Figure 1, along with those of the reference RRP and PIT wires. Below we take the fields at 10% and 90% of the normal state resistances as B_{irr} and B_{c2} , respectively.

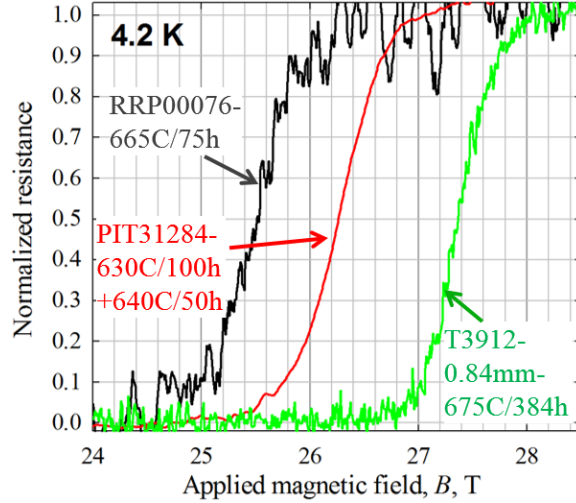


Figure 1. The R - B curves of an APC wire as well as the reference RRP and PIT wires at 4.2 K.

The B_{irr} and B_{c2} values of the RRP wire were ~ 25 and ~ 26 T, respectively, which are typical for RRP wires reacted at 665°C . The standard PIT wire had B_{irr} and B_{c2} values of 25.8 and 26.7 T, respectively, which are similar to what Godeke measured for PIT wires reacted at 675°C [24] and are nearly 1 T higher than those of the RRP wire. The B_{irr} and B_{c2} values (4.2 K) of T3912-0.84mm- $675^{\circ}\text{C}/384\text{h}$ were 27 and 27.8 T, respectively, over 1 T higher than those of the standard PIT wire. These results confirm our previous measurements in late 2018 ([22]) showing that the ternary APC wires have higher B_{irr} and B_{c2} than the standard PIT and RRP conductors.

The measured $J_{c,non-Cu}$ values of the reference wires as well as T3912 given various heat treatments are shown in Figure 2, along with the FCC $J_{c,non-Cu}$ specification [3]. Here it is worth mentioning that the FCC $J_{c,non-Cu}$ specification is not just a single value at specifically 16 T, but rather a $J_{c,non-Cu}$ - B curve that can be generated by a set of parameters given in [3]: this is because producing a 16 T bore field (which leads to a slightly higher peak field on the conductors [3]) in fact requires the use of $J_{c,non-Cu}$ at a higher field for the magnet design (e.g., ~ 19 T for a 14%

margin [3] along the load line). In fact, a calculation of conductor temperature margin can show that the $J_{c,non-Cu}$ at 19 T is more relevant for a 16 T magnet than the $J_{c,non-Cu}$ at 16 T is. The 16 T $J_{c,non-Cu}$ values of the RRP and PIT wires were 1090 and 1005 A/mm², and the 19 T values were 395 and 450 A/mm², respectively. These are not the highest values that top-performing RRP and PIT wires can reach (which are around 1300 A/mm² at 16 T [2]), but they are in the typical $J_{c,non-Cu}$ spectrum of RRP and PIT wires. Despite lower $J_{c,non-Cu}$ values at low fields, PIT wires outperform RRP wires at high fields (19 T and above) due to higher B_{irr} , which has also been seen previously [2]. Because the I_c values of the APC wires with 0.84 mm diameter could not be obtained at low fields due to quenching during the $V-I$ tests (which could be due to large subelement size D_s and a bit too long reaction time), the $J_{c,non-Cu}-B$ data are fitted with a commonly-used two-component pinning force model, which has been shown by a number of studies to work well for both standard and APC wires [10,18,22]. As can be seen in Figure 2, the fittings to the data are good. The $J_{c,non-Cu}$ of T3912 at 0.71 mm diameter (with D_s of 70 μ m) after a HT of 700°C/71h was 3% lower than the FCC $J_{c,non-Cu}$ specification at 16 T, but surpassed the latter at 19 T and above. The RRR of this wire was 85. Improvement of RRR requires further improvement of wire quality as well as HT optimization studies to prevent too long reaction time. With the same HT temperature of 700°C, an increase of the wire diameter to 0.84 mm (with D_s of 83 μ m) led to only slightly higher $J_{c,non-Cu}$. On the other hand, lower HT temperatures led to substantially higher $J_{c,non-Cu}$: e.g., reducing HT to 685°C increased the $J_{c,non-Cu}$ to 730 A/mm² at 19 T (i.e., 13% higher than the FCC specification) and 1600 A/mm² (extrapolated value) at 16 T. Further reducing HT to 675°C led to even higher $J_{c,non-Cu}$: e.g., 390 A/mm² at 21 T (i.e., 29% higher than the FCC specification), and an extrapolated value of 1740 A/mm² at 16 T, which is 16% higher than the FCC specification and about 30% higher than RRP record.

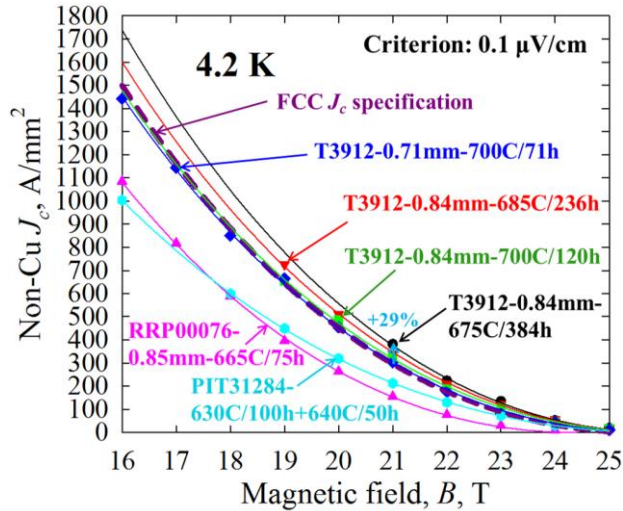


Figure 2. Non-Cu J_c s of the reference wires and the APC wires, as well as the FCC $J_{c,non-Cu}$ specification.

4. Discussions

In addition to the high B_{irr} and B_{c2} , we found that APC wires also had higher Sn content in the FG layers as compared to that seen in conventional wires. The Sn concentrations of T3912 as well as those of several other wires fabricated at Hyper Tech were measured by EDS – these wires were carefully selected so that they have different combinations of Zr, Ta, and O: (1) T3736 used a Nb-7.5wt.%Ta tube and a Cu-clad Sn rod in the core (i.e., T3736 has Ta but no Zr or O), (2) T3739 used a Nb-1wt.%Zr tube and a mixture of Cu, Sn, and SnO₂ powders in the core that gives sufficient oxygen (i.e., T3739 has Zr and O but no Ta), (3) T3814 used a Nb-1wt.%Zr-7.5wt.%Ta tube and a mixture of Cu and Sn powders in the core (i.e., T3814 has Zr and Ta but no O), and (4) T3843 used a Nb-7.5%Ta tube and a mixture of Cu, Sn, and SnO₂ powders in the core (i.e., T3843 has Ta and O but no Zr). The measured Sn concentrations of the Nb₃Sn layers in these wires are shown in Figure 3. For all of the samples, the first EDS measurement spots

were in the coarse-grain (CG) A15 regions (which are known to have Sn content around 25 at.% [25]), and the last measurement spots were close to the FG/Nb interface, while all the other spots were in the FG layers. It can be seen that T3736, T3814, and T3843 generally had Sn concentrations in the FG layers between 22.5 and 24 at.%, which are typical for standard Nb₃Sn wires [25]. On the other hand, T3739 and T3912 had Sn concentrations in the FG layers between 24 and 25 at.%, close to stoichiometry. By comparing these five wires, it can be clearly seen that only the internally oxidized samples (Zr+O) had the highest Sn content in the Nb₃Sn layer. To verify the Sn content results, several APC and standard PIT and tube type wires using the same HT (675°C/120h) were sent to Ian Pong at Lawrence Berkley National Laboratory (LBNL) for an independent EDS study. The results of detailed line-scan measurements by Pong confirmed that the Sn concentrations of the APC wires were 1-1.5 at.% higher than those of standard wires [26].

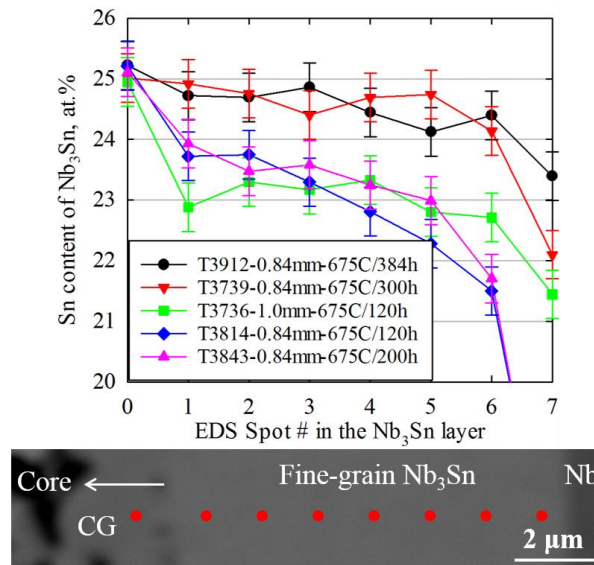


Figure 3. Sn concentrations in Nb₃Sn layers of the five wires and a schematic showing the EDS spots.

It is well established that the B_{irr} and B_{c2} of Nb_3Sn depend on its composition: for binary Nb_3Sn , B_{c2} increases with Sn content monotonically until 24.5 at.%, after which there is a sharp drop, which is arguably due to tetragonal transformation at low temperature [27]. Based on this, it is possible that the low B_{irr} values in binary APC wires (18-20 T [16,18]) were not only due to lack of ternary doping, but also because of their Sn content being near to 25 at.%. On the other hand, the addition of ternary dopants suppresses the tetragonal transformation, and thus prevents the sharp B_{c2} drop [27]. Therefore, with Ta dopant, the higher Sn content in the APC wires could be why they have higher B_{irr} and B_{c2} than standard PIT and RRP wires. It is worth mentioning that Ti doping may influence B_{c2} in a different way from Ta doping regarding Sn content due to possible different site occupancy (see a recent study [28] for example). All the standard PIT wires and our multifilamentary APC wires are based on Ta doping.

High Sn content in the Nb_3Sn layer is a unique feature of APC wires based on internal oxidation, and does not exist in standard wires. So, what could be the root cause of this phenomenon? In fact, a recently developed theory [5,29] explains this. This theory was developed for the diffusion reaction process of Nb_3Sn layer growth in a Sn-source/ Nb_3Sn / Nb system, which describes a Nb_3Sn filament during heat treatment. It proposes that the composition of the Nb_3Sn layer is determined by both thermodynamics and kinetics. With respect to the thermodynamic aspect, this theory analyzes the relation between Sn content and chemical potential of Sn (μ_{Sn}) for both Nb_3Sn and Sn sources (which could be a Cu-Sn alloy, Nb_6Sn_5 , etc.), because the μ_{Sn} of the Nb_3Sn layer is limited by the μ_{Sn} of its Sn source. The thermodynamic part of this theory explains qualitatively why different types of wires (RRP, PIT, bronze-process, etc.) have different Nb_3Sn composition features (see [5] for details). Thermodynamics determines the maximum limits of μ_{Sn} (and thus Sn content) in the Nb_3Sn layer, while kinetics determines how

far in reality the μ_{Sn} (and thus Sn content) are actually below these limits. With respect to the kinetic part, this theory analyzes the Nb₃Sn growth process, and proposes that there are two competing processes that determine the Sn content in the Nb₃Sn layer: one is the reaction at the Nb₃Sn/Nb interface which forms new Nb₃Sn layers but also produces Sn vacancies in the Nb₃Sn layer at the interface, and the other is the process of Sn atoms from the Sn source diffusing along the Nb₃Sn grain boundaries to the Nb₃Sn/Nb interface and filling the Sn vacancies (see [5] for a detailed description). Clearly, a faster reaction process relative to the diffusion process would leave a higher concentration of Sn vacancies remaining in the Nb₃Sn layer while the Nb₃Sn/Nb interface advances. Due to the extremely low bulk diffusivity of Sn inside the Nb₃Sn grains [30], unfilled Sn vacancies would be frozen within the Nb₃Sn lattice (which might transform to Nb-on-Sn anti-sites [31]) and lead to low Sn content in the formed Nb₃Sn. The internal oxidation in APC wires influences both processes. First, it refines Nb₃Sn grain size, and thus provides more paths for Sn diffusion, which is expected to promote the diffusion process. On the other hand, it has been found in the APC wires that internal oxidation reduces the Nb₃Sn layer growth rate (see [16] for a detailed study). Since, as noted above, the refined grain structure in internally oxidized A15 should enhance the diffusion process, the decreased Nb₃Sn layer growth rate indicates that the reaction rate at the Nb₃Sn/Nb interface must be suppressed for some reason. One possibility is this: similar to the fact that ZrO₂ particles sitting at Nb₃Sn grain boundaries can drag them and slow down their migration and thus suppress grain growth, the ZrO₂ particles at or adjacent to the Nb₃Sn/Nb interface may also slow down its forward motion. According to the above theory, if internal oxidation in the APC wires promotes the Sn diffusion process while suppressing the reaction process at the Nb₃Sn/Nb interface, it should lead to improved Sn contents within the FG

Nb₃Sn layer. Of course, although this theory can explain a few phenomena [5], it still requires further experimental work for validation.

BSE images of cross sections of T3912-0.71mm-700°C/71h and T3912-0.84mm-675°C/384h are shown in Figure 4. From these images the average area fractions of FG, residual Nb, and CG in filaments of both wires were calculated and are shown in Table 1, along with those of the T3882-0.84mm-675°C/330h [22] as well as those of standard PIT conductors. In Nb₃Sn wires, only the FG layers can carry supercurrents, while the CG cannot. From Table 1, the FG fractions of both T3912 wires are nearly 50% higher than that of the T3882-0.84mm-675°C/330h: this is the primary reason for the much higher $J_{c,non-Cu}$ of T3912 in comparison to T3882; a secondary reason is an improvement of wire uniformity (T3882 had a number of filaments with insufficient oxygen [22]). Since T3912-0.84mm-675°C/384h has lower FG fractions than T3912-0.71mm-700°C/71h, its higher $J_{c,non-Cu}$ is most likely due to higher flux pinning as a result of the lower reaction temperature. The residual Nb fractions of both T3912 wires (34%) are still much higher than those of standard PIT wires (typically 25% or below [23]). A closer analysis of the recipe of T3912 reveals that this is because it has too low of a Sn/Nb ratio – this means that the APC wires still have the potential to form more FG by converting more Nb via properly tweaking the recipe design, which is expected to lead to higher $J_{c,non-Cu}$.

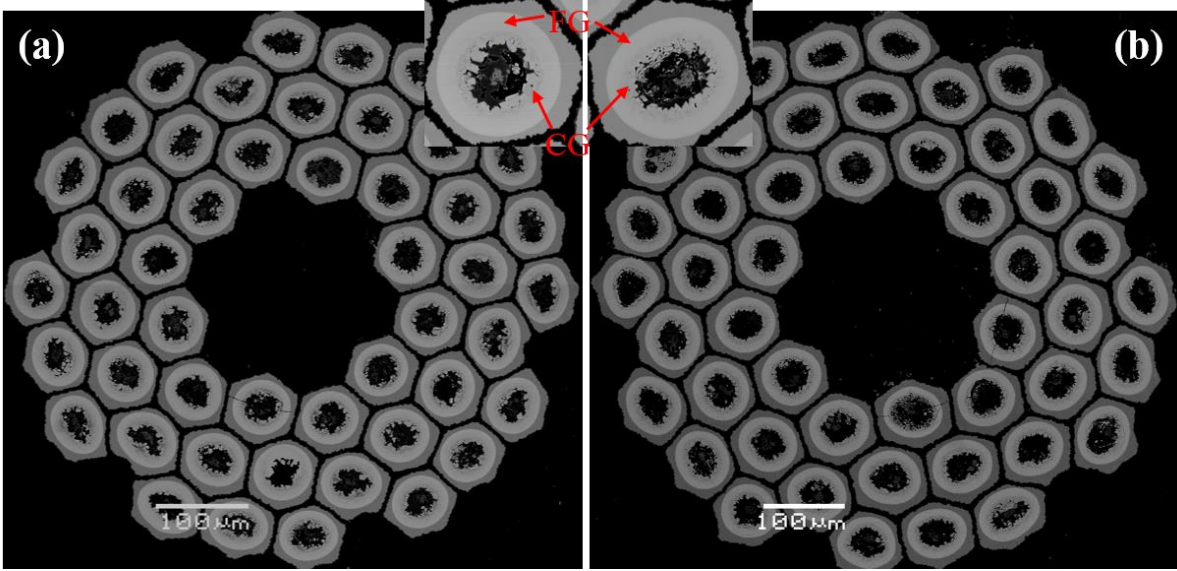


Figure 4. BSE images of cross sections for (a) T3912-0.71mm-700°C/71h, and (b) T3912-0.84mm-675°C/384h.

Table 1. Area fractions in filaments of T3882 and T3912 wires as well as standard PIT wires

Areas	T3882-0.84mm-675°C/330h [22]	T3912-0.71mm-700°C/71h	T3912-0.84mm-675°C/384h	Standard PIT [23]
Fine-grain A15	22%	33%	31.4%	40%
Residual Nb	45%	34%	34%	25%
Coarse-grain A15	13%	13.5%	15.7%	13.3%

Despite achievement of new record $J_{c,non-Cu}$ that is above the FCC specification, there is still much work to be done. First, it is necessary to continue to optimize the wire recipe, which on one hand may lead to better Nb/Sn and Cu/Sn ratios for a fuller reaction and thus higher $J_{c,non-Cu}$, and on the other hand will also likely further improve wire quality and thus RRR, considering that recipe optimization has been the primary contributor to the improvement of APC wire quality (e.g., filament shape) in the past two years. Second, it is important to continue to optimize the HT of the APC wires because a lower HT temperature benefits $J_{c,non-Cu}$ and proper reaction times

are required to retain high RRR. Since the grain size in the APC wires is small, the inverted multistage HT proposed by Segal [23] can also be used to reduce CG and form more FG. Third, exploration of some wire design variants that have been demonstrated in standard PIT wires could be very helpful in improving performance of the APC-PIT wires, such as the use of round filaments instead of the present hexagonal ones (this improves $J_{c,non-Cu}$ because it allows more Nb to be converted into Nb₃Sn without poisoning the RRR) and the use of a bundle barrier (which is effective in preserving high RRR) [32]. Next, it is necessary to continue the fabrication and optimization of 217-filament wires, which are important for reduction of D_s and thus improvement of conductor stability. We have fabricated a wire with 217 filaments using a Nb-0.6wt.%Zr-7.5wt.%Ta tube, which was drawn to 0.71 mm diameter (with D_s of 35 μ m) without wire breakage. A next logical step would be fabrication of wires with 217 filaments using Nb-1wt.%Zr-7.5wt.%Ta tubes for higher $J_{c,non-Cu}$. Here it is worth mentioning that APC wires demonstrate good drawability: all the APC wires of the past 23 billets (including 13 using Nb-0.6wt.%Zr-7.5wt.%Ta tubes and 10 using Nb-1wt.%Zr-7.5wt.%Ta tubes) were drawn to 0.5-0.84 mm diameters in single pieces without any wire breakage. In parallel with the above research and development tasks, there are other tasks which are needed in order to push APC wires towards practical, magnet-grade conductors, such as process improvement and increased billet size, etc., as well as evaluation of electro-mechanical properties (e.g., uniaxial tensile and transverse pressure tests), which are important for magnet applications.

5. Conclusions

Our results reported here on multifilamentary APC Nb₃Sn conductors confirm the high B_{irr} and B_{c2} of ternary, internal oxidation route APC wires (27-28 T at 4.2 K), which are 1-2 T higher

than RRP and standard PIT wires. This is because APC wires have significantly higher Sn content in the Nb₃Sn layer as compared to those without internal oxidation, which can be explained using a diffusion reaction theory. The $J_{c,non-Cu}$ values of these recent APC wires have broken the Nb₃Sn $J_{c,non-Cu}$ record that stood for nearly two decades, and have met the FCC conductor $J_{c,non-Cu}$ specification. It was found that lower HT temperature benefits $J_{c,non-Cu}$: a heat treatment at 675°C led to a $J_{c,non-Cu}$ that was 29% higher than the FCC specification at 21 T. Analysis of SEM images showed that the FG Nb₃Sn fractions had been increased dramatically, but are still below what we estimate is possible for properly optimized wire chemistries. Finally, some work remains to be done in order to further improve performance of such wires and push them towards practical conductors, and we see a potentially viable path to make magnet-grade, long-length APC Nb₃Sn conductors.

Acknowledgements

This work is supported by the Laboratory Directed Research and Development (LDRD) program of Fermi National Accelerator Laboratory and Hyper Tech SBIR DE-SC0013849 and DE-SC0017755 by US Department of Energy. Some tests were performed at the NHMFL, which is supported by National Science Foundation Cooperative Agreement No. DMR-1644779 and the State of Florida. The measurements at the NHMFL were greatly helped by Jan Jaroszynski, Griffin Bradford, and Yavuz Oz. We are grateful to ASC of the NHMFL for letting us use the I_c transport test system. We thank Ian Pong from LBNL for supplying the RRP and PIT wires that are used as references in this work, and for the independent EDS studies that confirmed our results. We acknowledge some discussions under the U.S. Magnet Development Program context, which benefit this project a lot.

References

- [1]. Benedikt M and Zimmermann F 2016 Status of the future circular collider study *CERN-ACC-2016-0331*
- [2]. Ballarino A and Bottura L 2015 Targets for R&D on Nb₃Sn Conductor for High Energy Physics *IEEE Trans. Appl. Supercond.* **25** 6000906
- [3]. Tommasini D and Toral F 2016 Overview of magnet design options *EuroCirCol-P1-WP5 report* 4-6
- [4]. Cooley L D, Ghosh A K, Dietderich D R and Pong I 2017 Conductor Specification and Validation for High-Luminosity LHC Quadrupole Magnets *IEEE Trans. Appl. Supercond.* **27** 6000505
- [5]. Xu X 2017 A review and prospects for Nb₃Sn superconductor development *Supercond. Sci. Technol.* **30** 093001
- [6]. Parrell J A, Zhang Y Z, Field M B, Cisek P and Hong S 2003 High field Nb₃Sn conductor development at Oxford Superconducting Technology *IEEE Trans. Appl. Supercond.* **13** 3470-3
- [7]. Tarantini C, Lee P J, Craig N, Ghosh A and Larbalestier D C 2015 Examination of the trade-off between intrinsic and extrinsic properties in the optimization of a modern internal tin Nb₃Sn conductor *Supercond. Sci. Technol.* **28** 099501
- [8]. Flukiger R, Specking W, Klemm M and Gauss S 1989 Composite core Nb₃Sn wires: preparation and characterization *IEEE Trans. Magn.* **25** 2192-9
- [9]. Zhou R, Hong S, Marancik W and Kear B 1993 Artificial flux pinning in Nb and Nb₃Sn superconductors *IEEE Trans. Appl. Supercond.* **3** 986-9
- [10]. Rodrigues D, Da Silva L B S, Rodrigues C A, Oliveira N F and Bormio-Nunes C 2011 Optimization of Heat Treatment Profiles Applied to Nanometric-Scale Nb₃Sn Wires With Cu-Sn Artificial Pinning Centers *IEEE Trans. Appl. Supercon.* **21** 3150-3
- [11]. Zeitlin B A, Marte J, Ellis D, Benz M and Gregory E 2003 Some Effects of the Addition of 1 at% Zr to Nb on the Properties and Ease of Manufacture of Internal-Tin Nb₃Sn *Adv. Cryog. Eng.* **50B** 895-902
- [12]. Zeitlin B A, Gregory E, Marte J, Benz M, Pyon T, Scanlan R and Dietderich D 2005 Results on Mono Element Internal Tin Nb₃Sn Conductors (MEIT) with Nb_{7.5}Ta and Nb(1Zr+O_x) Filaments *IEEE Trans. Appl. Supercond.* **15** 3393-6
- [13]. Motowidlo L R, Lee P J and Larbalestier D C 2009 The Effect of Second Phase Additions on the Microstructure and Bulk Pinning Force in Nb₃Sn PIT Wire *IEEE Trans. Appl. Supercond.* **19** 2568-72
- [14]. Xu X, Sumption M D, Peng X and Collings E W 2014 Refinement of Nb₃Sn grain size by the generation of ZrO₂ precipitates in Nb₃Sn wires *Appl. Phys. Lett.* **104** 082602
- [15]. Benz M G 1968 The superconducting performance of diffusion processed Nb₃Sn doped with ZrO₂ particles *Trans. of Met. Soc. of AIME* **242** 1067-70
- [16]. Xu X, Sumption M D and Peng X 2015 Internally Oxidized Nb₃Sn Superconductor with Very Fine Grain Size and High Critical Current Density *Adv. Mater.* **27** 1346-50
- [17]. Xu X, Sumption M D and Peng X 2018 Superconducting wires and methods of making thereof *U.S. Patent 9916919*, filed date: Feb. 18, 2015

- [18]. Motowidlo L, Lee P J, Tarantini C, Balachandran S, Ghosh A and Larbalestier D C 2017 An intermetallic powder-in-tube approach to increased flux-pinning in Nb₃Sn by internal oxidation of Zr *Supercond. Sci. Technol.* **31** 014002
- [19]. Xu X, Peng X, Sumption M D and Collings E W 2017 Recent Progress in Application of Internal Oxidation Technique in Nb₃Sn Strands *IEEE Trans. Appl. Supercond.* **27** 6000105
- [20]. Balachandran S, Tarantini C, Lee P J, Kametani F, Su Y, Walker B, Starch W L and Larbalestier D C 2019 Beneficial influence of Hf and Zr additions to Nb₄at.%Ta on the vortex pinning of Nb₃Sn with and without an O Source *Supercond. Sci. Technol.* **32** 044006
- [21]. Buta F, Bonura M, Matera D, Ballarino A, Hopkins S, Bordini B and Senatore C 2018 Properties and microstructure of binary and ternary Nb₃Sn superconductors with internally oxidized ZrO₂ nanoparticles *Applied Supercond. Conf.* 1MPo2A-06
- [22]. Xu X, Rochester J, Peng X, Sumption M D and Tomsic M 2019 Ternary Nb₃Sn conductors with artificial pinning centers and high upper critical fields *Supercond. Sci. Technol.* **32** 02LT01
- [23]. Segal C, Tarantini C, Lee P J and Larbalestier D C 2017 Improvement of small to large grain A15 ratio in Nb₃Sn PIT wires by inverted multistage heat treatments *IOP Conf. Ser. Mater. Sci. Eng.* **279** 012019
- [24]. Godeke A, Jewell M, Fischer C, Squitieri A, Lee P and Larbalestier D 2005 The upper critical field of filamentary Nb₃Sn conductors *J. Appl. Phys.* **97** 093909
- [25]. Hawes C D, Lee P J and Larbalestier D C 2006 Superconductor Science and Technology Measurements of the microstructural, microchemical and transition temperature gradients of A15 layers in a high-performance Nb₃Sn powder-in-tube superconducting strand *Supercond. Sci. Technol.* **19** S27-37
- [26]. Pong I, unpublished data
- [27]. Suenaga M, Welch D O, Sabatini R L, Kammerer O F and Okuda S 1986 Superconducting Critical-Temperatures, Critical Magnetic-Fields, Lattice-Parameters, and Chemical-Compositions of Bulk Pure and Alloyed Nb₃Sn Produced by the Bronze Process *J. Appl. Phys.* **59** 840-53
- [28]. Heald S M, Tarantini C, Lee P J, Brown M D, Sung Z, Ghosh A K and Larbalestier D C 2018 Evidence from EXAFS for Different Ta/Ti Site Occupancy in High Critical Current Density Nb₃Sn Superconductor Wires. *Sci. Rep.* **8** 4798
- [29]. Xu X and Sumption M 2016 A model for the compositions of non-stoichiometric intermediate phases formed by diffusion reactions, and its application to Nb₃Sn superconductors *Sci. Rep.* **6** 19096
- [30]. Muller H and Schneider Th 2008 Heat treatment of Nb₃Sn conductors *Cryogenics.* **48** 323-30
- [31]. Besson R, Guyot S and Legris A 2007 Atomic-scale study of diffusion in A15 Nb₃Sn *Phys. Rev. B* **75** 054105
- [32]. Bordini B, Ballarino A, Macchini M, Richter D, Sailer B, Thoener M and Schlenga K 2017 The Bundle-Barrier PIT Wire Developed for the HiLumi LHC Project *IEEE Trans. Appl. Supercond.* **27** 6000706